Flexible Runway Scheduling With Non-Linear Noise Restrictions Using a Tabu Search Algorithm

Roling, P.C.; Hyde, E.J.A.

DOI
10.2514/6.2024-4082

Publication date
2024

Document Version
Final published version

Published in
AIAA Aviation Forum and ASCEND, 2024

AIAA Aviation Forum and ASCEND co-located Conference Proceedings
29 July - 2 August 2024, Las Vegas, Nevada
AIAA AVIATION FORUM AND ASCEND 2024
10.2514/6.2024-4082

Flexible runway scheduling with non-linear noise restrictions using a Tabu search algorithm

Paul C. Roling[1] and Sam Lagerwij[2]
Delft University of Technology

In response to the growing demand for air travel, major airports are approaching critical thresholds in their infrastructure capacity. As the transportation sector continues to expand, it is increasingly important to address environmental concerns that arise from aspects, such as noise annoyance and fuel consumption. This paper aims to enhance the existing Flexible Runway Scheduling Model (FRSM) by integrating a tabu search algorithm with Receding Horizon Control (RHC), introducing non-linear noise restrictions, and implementing more sophisticated fuel burn modeling. The main goal is to evaluate how certain improvements affect the FRSM. To achieve this, a methodology has been developed that uses a multi-objective tabu search algorithm to minimize both fuel consumption and noise annoyance while assigning flights to runways. This study provides a comprehensive analysis of Amsterdam Airport Schiphol (AAS) across different scenarios, ranging from a 1.5-hour flight schedule to a full-day simulation, revealing significant findings. For the 1.5-hour and six-hour scenarios, the tabu search algorithm achieves a 55% and 87.3% reduction in computational time with marginal losses of 0.73% and 0.19% in solution accuracy for fuel burn optimization. Throughout all scenarios, the tabu search algorithm consistently results in a reduction of highly annoyed individuals ranging from 2.14% up to 62.5% compared to the existing FRSM, demonstrating its effectiveness. Moreover, the algorithm minimizes the impact on the flight schedule in terms of delay. Notably, as the flight schedule length increases, the performance of the tabu search algorithm improves compared to the existing FRSM. A sensitivity analysis optimization horizon indicates a positive effect on results, albeit with an associated computational cost. In conclusion, this study showcases the positive impacts of the remodeled FRSM, enabling a faster and more accurate trade-off. The research findings provide valuable insights for optimizing runway scheduling at major airports while balancing efficiency gains with environmental considerations.

I. Introduction

The growth of the aviation sector has a direct influence on the operations of airports. As the demand for flying increases, the number of operations performed at an airport increases with it. To cope with the increasing operations, several factors and expansion possibilities can be considered while ensuring capacity, safety and regulations.

As physical growth of the airport is often not possible due to local restrictions, airports turn to other possibilities to optimize their operations given the current infrastructure. One of the biggest contributors to airport capacity is the runway capacity which is defined by Neufville as: "the expected number of movements in a time period on a runway system without violating Air Traffic Management (ATM) rules, assuming continuous demand"[1]. To improve runway capacity, several studies in different research areas have been performed. The RECAT-EU scheme is one of those results and is a revised separation scheme[2,3].

Noise disturbance has become a topic of discussion in the expansion of airport operations[4]. Airports operating under noise restrictions often follow a preferred runway list according to regulations and agreements with (local)

[1] Lecturer / researcher. AIAA member
[2] MSc student, Air Transport Operations

governments. These preferred sequences together with ICAO noise abatement procedures ensure noise disturbance is limited but not negligible[5,6]. This noise disturbance is limited by legislation in different ways, either by limiting the noise at certain locations, the size of contours, the number of people or houses withing a contour or even using dose response relationships to determine a statistical number of people who will be annoyed or sleep disturbed. Especially the latter require non-linear equations to calculate and cannot be incorporated in the current model[7].

II.Model

Figure 1 gives an overview of the model and input and the steps needed to come to a solution.

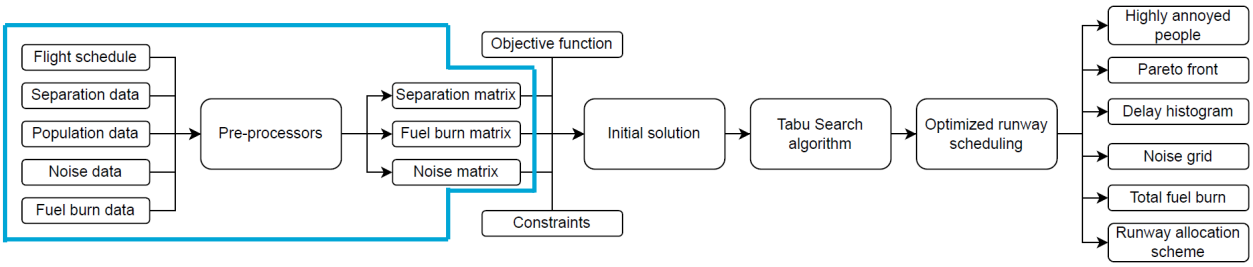

Figure 1: model overview

A. Separation modelling

The most dominant factor influencing runway capacity is the minimum separation requirement between Operations[8]. The minimum separation time is dependent on several parameters such as i) operation type, ii) weight class and iii) runway use.

The separation modeling is based on previous research[7,14] where the separation is determined by considering a leading and following aircraft. Four distinct combinations on a single runway arise from these aircraft: two consecutive arrivals, two consecutive departures, an arrival followed by a departure, and a departure followed by an arrival. For these combinations, different equations are applied to calculate the separation time, which varies based on the specific runways in use.

1. The required time separations between two arrivals, where the trailing aircraft (j) is faster and hence minimum separation distance ($s_{i,j}$) is when the first aircraft (i) touches down. The time separation is the time the trailing aircraft needs to traverse that distance, which is equal to that distance divided by the speed of the trailing aircraft (V_j), or the runway occupancy time of the first aircraft ($AROT_i$), whichever is larger.

$$T_{i,j} = \max\left[\frac{s_{ij}}{V_j}, AROT_i\right] \quad (1)$$

2. When the trailing aircraft is slower, the minimum separation is when the leading aircraft (i) intercepts the common path at distance n from the landing threshold. The leading aircraft then lands the distance n divided the speed (V_i) later. The trailing aircraft lands distance n plus the required airborne separation (s_{ij}) both divided by its speeds (V_j). the time separation is then the difference, or the runway occupancy of the first aircraft ($AROT_i$), whichever is larger.

$$T_{i,j} = \max\left[\frac{n+s_{ij}}{V_j} - \frac{n}{V_i}, AROT_i\right] \quad (2)$$

3. When two aircraft land in opposite directions, the minimum time separation is determined by the required distance when the first aircraft would do a go around just before touchdown. The second aircraft must then at least be at maneuvering altitude (MVA). The time from that point to touch down is then given by the MVA divided by the rate of descent (ROC_j) plus a communications buffer.

$$T_{i,j} = \frac{MVA}{ROD_j} + \overline{c} \quad (3)$$

4. When two aircraft depart in succession in the same direction, the minimum time separation is only based on time (TBS_{ij}), as aircraft can be diverted quickly after take-0ff, and the runway occupancy time of the first aircraft ($DROT_i$).

$$T_{i,j} = \max\left[TBS_{ij}, DROT_i\right] \quad (4)$$

5. When two aircraft depart in opposite direction, airborne separation is not required, and the second aircraft can line up and depart when the first aircraft has left the runway ($DROT_i$).

$$T_{i,j} = DROT_i \quad (4)$$

6. When a departure takes place after an arrival in the same runway direction, the departing aircraft can line up and take off after the landing aircraft has left the runway ($AROT_i$).

$$T_{i,j} = AROT_i \quad (5)$$

7. The longest time separation is required when an arrival comes after a departure in the opposite direction. The total time is equal to the departure taking off ($DROT_i$), climbing to the minimum vectoring altitude (MVA) and then the arriving aircraft descending from minimum vectoring altitude to the touchdown point, assuming the rate of climb (ROC) is much higher than the rate of descent (ROD) and thus no airborne separation is required.

$$T_{i,j} = \frac{MVA}{ROD} + DROT_i + \frac{MVA}{ROC} \quad (6)$$

At airports where runways are closely situated or dependencies arise from trajectory intersections, additional separation requirements are introduced.[14]

B. Fuel Burn Modeling

As the model will make a trade-off between fuel burn and noise disturbance, accurate modeling of both is important. In this research a method is proposed for the fuel burn calculation which is based on previous research performed by Delsen[9] and parameters obtained from the Base of Aircraft Data (BADA)[10].

To calculate the fuel burn of a flight the flight path is divided into several stages for which the individual fuel burn is calculated. The total fuel burn (TFB) calculation (eq. 7) is expressed in kilograms of kerosene. The fuel burn per segment (TFBS) is then calculated (eq. 8):

$$TFB = \sum_{s \epsilon S} TFB_s \quad (7)$$

$$TFB_s = \frac{D \cdot \dot{m}_f}{V_{TAS}} \quad (8)$$

The distance per segment (D) can be obtained from Aeronautical Information Packages[11] which are provided per airport. The fuel flow (m_f) in [kg/s] is obtained from AEDT, which provides coefficients of all types of aircraft which are currently in use. The fuel flow is thrust dependent and can be obtained assuming a thrust specific fuel consumption:

$$\dot{m}_f = C_T \cdot T_{hr} \quad (10)$$

For the jet and turboprop engines, the thrust specific fuel consumption, C_T, is obtained according to Equation 11 for jet engines, and Equation 12 for turboprop engines. C_T is a function of true airspeed, V_{TAS}, and the aircraft and engine dependent coefficients C_{f1} and C_{f2}.

$$C_T = C_{f1}\left(1 + \frac{V_{TAS}}{C_{f2}}\right) \quad (11)$$

$$C_T = C_{f1}\left(1 - \frac{V_{TAS}}{C_{f2}}\right)\left(\frac{V_{TAS}}{1000}\right) \quad (12)$$

In this research the segments for arriving aircraft are divided into four parts: i) the holding just before the Initial Approach Fix (IAF), ii) the segment from the IAF to the Final Approach Fix (FAF), iii) the segment from the FAF to the runway and iv) the segment from the runway to the pier. For departing aircraft, the segments are divided in two parts: i) the segment from the pier to the runway and ii) from the runway to the first waypoint on the Standard Instrument Departure (SID).

The model can assign delays to aircraft if necessary. This delay comes at the cost of additional fuel consumption and must be incorporated in the model as well. For arriving aircraft, it is assumed that the initial few minutes of delay take place after the IAF, while further delay will be accumulated in a holding pattern with a slightly higher fuel flow due to making turns. The fuel flow is taken as the cost per second of delay for arriving aircraft. For departing aircraft, it is assumed that the fuel burn during the taxi phase is extended. In the model, taxi thrust is assumed to be 7% of total thrust[12] from which the fuel flow can be calculated with previous equations.

C. Noise Modeling

The second objective is to limit noise disturbance. As fly-over noise is a non-stationary signal, the duration of the sound has to be taken into account. For this, the Sound Exposure Level (SEL or LAE) can be used (eq 12). The instantaneous A-weighted sound pressure level is indicated by L_A. The integration time is replaced with a reference time of $T_1 = 1$s.

$$SEL = 10\log\left[\frac{1}{T_0}\int_0^T 10^{\frac{L_A(t)}{10}}\,dt\right] \tag{13}$$

To use the equation in a linear optimization problem, the logarithmic parts of the equation must be adjusted. For this, the Acoustic Energy Level (eq. 14) can be used.

$$AEL = \frac{E_n}{E_0} = 10^{\frac{SEL_n}{10}} \tag{14}$$

To capture the effect of noise in airport communities due to air traffic activities the day-evening-night level L_{DEN} noise metric is used. This metric is calculated via Equation 15, where T_{ref} indicates the period. The penalty associated with a noise event in the evening or night is represented by w_i. With a 5 dB penalty for noise during the evening (19.00-23.00), and a 10 dB penalty for noise during the night (23.00-7.00)[15]. By adding up the number of flights and the associated SEL value, the LDEN value can be computed.

$$L_{DEN} = 10\log\left[\sum_{i=1}^{n_{flights}} 10^{\frac{SEL+w_i}{10}}\right] - 10\log\left[\frac{T_{ref}}{T_0}\right] \tag{15}$$

To calculate the SEL for an aircraft operation a noise modeling program is used. In this research use is made of the Aviation Environmental Design Tool (AEDT) designed by the FAA[16]. By defining the group of aircraft of interest, a set of measurements can be obtained for every combination of runway, aircraft and STAR/SID for each individual grid point, as shown in figure 2. In this research it is assumed that the assigned delay does not imply extra noise disturbance. Delay is assigned at the IAFs or on the ground, not adding noise to the defined noise grid.

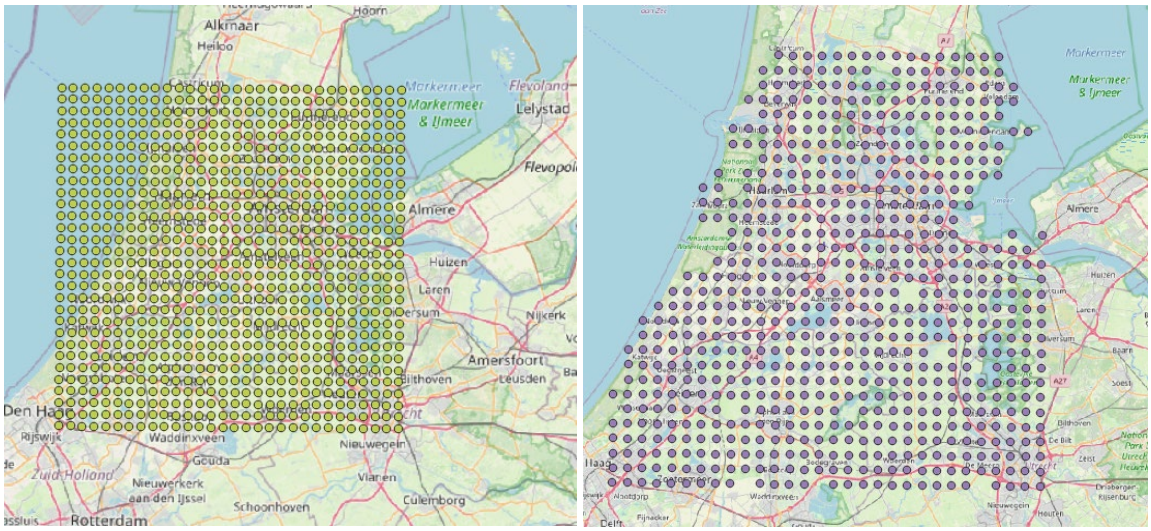

Figure 2: Noise grid (left) and population grid (right)for AMS

The current model lacks the incorporation of penalties for increased noise levels. To address this, a non-linear metric has been selected for this research. The metric measures the number of Highly Annoyed (HA) people and represents a dose-response relationship. It has been incorporated in the Dutch Aviation Act, which has formed the legal framework for AAS since 2003. This framework aims to restrict the environmental impact round the airport. This protection is provided by the "Criteria of equality", which restricts the number of HA people within L_{DEN} contours[17]. The limit value for the number of HA people within the 48 dB(A) L_{DEN} contour for AAS is 166,500, and 45,000 for the number of severely sleep-disturbed people (SDP) within the 40 dB(A) L_{night} contour[17].

To determine the number of annoyed people, three steps have been taken. Firstly, locations where the LDEN value is 48 dB(A) or above have been identified. Next, using Equation 16, the percentage of HA people has been calculated[18]. The L_{DEN} can be calculated using Equation 155. Finally, the percentage has been multiplied by the number of people living at the grid point. The total number of HA people has been determined by adding the number of HA people per grid point. The same procedure is used to determine the number of SDP. To obtain the percentage of SDP Equation 17 is used.

$$\%HAP = 1 - \frac{1}{\left[1 + e^{(-7.7130 + 0.1260 * L_{DEN})}\right]} \qquad (16)$$

$$\%SDP = 1 - \frac{1}{\left[1 + e^{(-6.2952 + 0.0960 * L_{night})}\right]} \qquad (17)$$

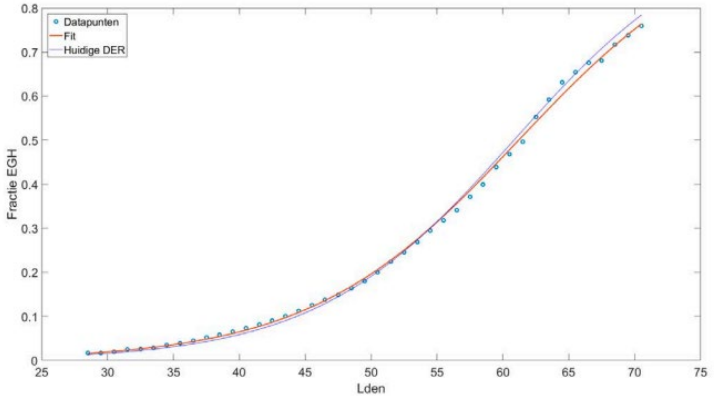

Figure 3: Dose response relationship

III.Solution methods

A. Mathematical formulation

Sets

F : Set of flights
R : Set of runway ends
P : Set of grid points

Binary variables

x_i^r : flight i uses runway r

y_{ij} : flight i takes place before flight j

g_{xy} : noise annoyance is reached at grid point x,y

Continuous variables

T_f : operating time of flight f

D_f : delay in the terminal movement area for arrivals or departure delay of flight f

Dh_f : Holding delay of flight f

D_{total} : sum of delay of all flights

HAP_{xy} : Highly annoyed people at grid point xy

Parameters

c_f^r : fuel burn for flight f with runway r

cd_f :delay fuel burn per second for flight f

ch_f : holding delay fuel burn per second for flight f

nf : normalization factor for fuel
nn : normalization factor for noise
S_{ij} : required separation between flight i and flight j

P_{xy} : People living at grid point xy

c_{opt} : small penalty
α : weight factor for fuel
β : weight factor for noise

Objective

$$\text{Min } Z = \alpha.nf \sum_{f \in F} \left[\left(\sum_{r \in R} c_f^r x_f^r \right) + cd_f D_f + ch_f Dh_f \right] + \beta.nf \sum_{xy \in P} HAP_{xy} + c_{opt} D_{total} \qquad (18)$$

The objective function, as described in Equation 18, consists of three terms. The first term aims to minimize fuel consumption when allocating runways to flights. This factor depends on the fuel cost associated with assigning flight f to runway r and incorporates a penalty for any delay assigned to the flight. As clarified in the fuel burn modeling section, this penalty escalates when the flight enters holding mode. The second term focuses on minimizing noise disturbance. If the L_{DEN} threshold of 48 dB(A) is surpassed, the cost of annoyance is determined by the number of highly annoyed people living at that specific grid point, represented by a non-linear relationship. The final component relates to total delay minimization. To ensure the assignment of all flights without excessively delaying any single flight or disproportionately scheduling flights on the most noise-preferred runway, a small penalty is integrated into the objective function. This inclusion ensures efficient and balanced runway scheduling.

As the problem is multi-objective and the two objectives have different units, a normalization has to be applied to both, indicated by n_f and n_n. Normalization is established by considering the range between the minimal and maximal solutions for both fuel and noise outcomes per window. This chosen range enables a dimensionless trade-off.

1. *Constraints*

$$\sum_{r \in R} x_f^r = 1, \forall f \in F \tag{19}$$

$$T_f - D_f - DH_f = TS_f, \forall f \in F \tag{20}$$

$$D_f \leq D_{f,\max}, \forall f \in F_{arr} \tag{21}$$

$$T_j - T_i - My_{ij} - Mx_i^r - Mx_j^{r'} \geq S_{ij}^{r,r'} - 3M, \forall i \in F, j \in F_{i'}, r, r' \in R \tag{22}$$

$$y_{ij} + y_{ji} = 1 \forall i \in F, j \in F_i \tag{23}$$

The first constraint (eq. 19) forces each flight to be assigned to exactly one runway end. The second constraint (eq 20) forces the landing or take of time to be equal to the earliest time plus the delay in the terminal movement area plus the holding delay for arrivals. The third constraint (eq. 21) limits the delay in the terminal movement area to a maximum amount for all arrivals.

The fourth constraint forces the time separation between one aircraft and another aircraft that can have a conflict with ($F_{i'}$) for all possible runway combinations and a given order of operation. The value of $S_{ij}^{r,r'}$ depends on the aircraft combinations and the runway combinations. Constraint 23 forces exactly one order possibility for each flight i and all flights j it can be swapped with (F_i).

B. Tabu search

A tabu search algorithm has been used in this research to evaluate the effect of a different solving method. The main goal is to solve the Flexible Runway Scheduling Model (FRSM) quicker and implement non-linear elements. The tabu search algorithm is a type of search method that focuses on finding a single solution[20] and can be used in a variety of optimization problems. However, it needs to be adjusted for each specific problem.

Initial Solution Generation

Starting with a viable solution can enhance both the outcome's quality and reduce the computational time required. Therefore, in this research, the initial solution is obtained through a greedy algorithm based on the dispatching (priority) rule. This rule, commonly used in machine scheduling, prioritizes jobs awaiting processing on a machine. This concept can be adapted to the context of FRSM, in which the runways serve as machines and the flights the jobs to be scheduled. When a runway becomes available, a dispatching rule inspects the waiting flights and selects the flight with the highest priority. These rules have proven to obtain a reasonably good solution in a relatively short time.

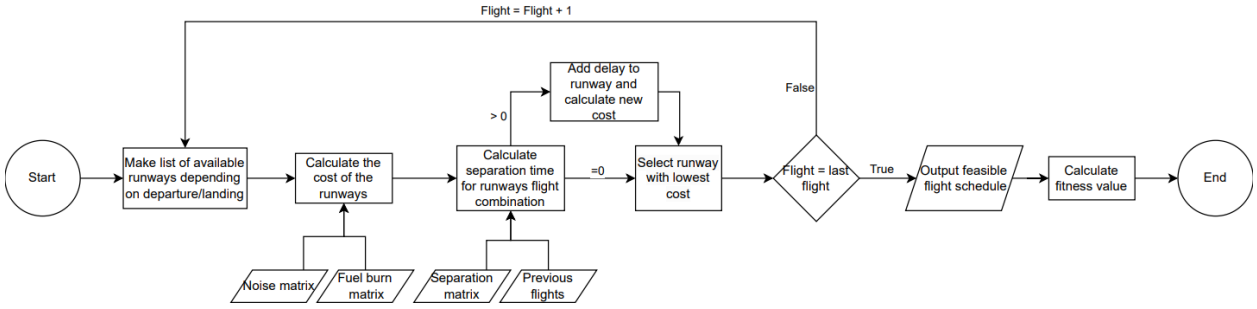

Figure 4: Initial solution generation

This approach is adapted for this research and is called the "Target Time First" greedy algorithm, illustrated in figure 4. In the algorithm, the flights are assigned to a runway in the order of ascending scheduled operating times. At each step, it looks for the most cost-efficient assignment for the unscheduled flight with the earliest scheduled operating time (SOT). While scheduling, it considers the assignment of previous flights. When all the flights are assigned to a runway the initial cost is computed and an initial feasible flight schedule is produced as the output.

Tabu search algorithm

The tabu search algorithm, shown in figure 5, is a widely employed metaheuristic method that incorporates intuitive concepts to guide the search process away from local optima. Its fundamental idea lies in maintaining a short-term memory, known as the "Tabu List". This list records recent moves or solutions, called "tabu moves", which are prohibited from being revisited in future moves. These moves are forbidden for a user-defined number of iterations. This mechanism prevents the algorithm from becoming trapped in local cycles or repeatedly revisiting sub-optimal solutions. However, there exists one exception for a tabu move: when such a move improves the best-known solution throughout the search. This exceptional scenario is recognized as an aspiration condition.

The search starts with the feasible initial solution and explores the solution space by making small modifications or moves to reach neighboring solutions. During the search process, the algorithm evaluates the quality of each neighbor using an objective function. It is not required that every new solution should be better than the previous solution. The algorithm continues with iterating until a stopping criterion is met, such as a fixed amount of CPU time, or a fixed number of consecutive iterations without improvement in the objective value. Furthermore, the algorithm stops when there are no feasible moves into the local neighborhood of the current trial solution.

The tabu search algorithm employs a comprehensive neighborhood generation

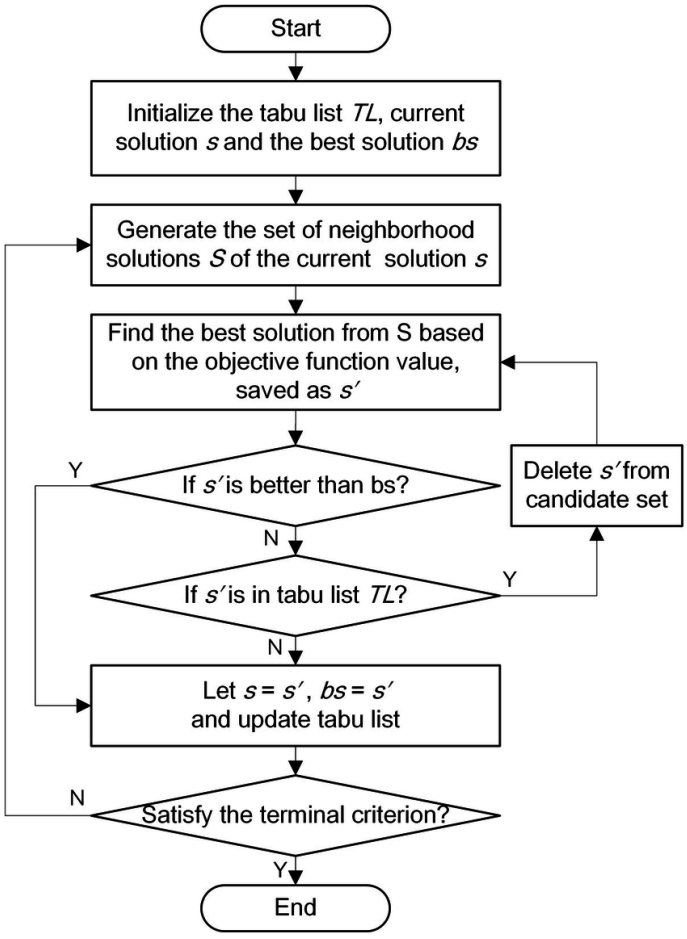

Figure 5: Tabu search algorithm

strategy centered on two key operations: swapping the order of flights and the reassignment of runways allocated to flights. This method is used to explore the solution space effectively. The swapping process allows the algorithm to explore various sequences of flights, aiming to minimize delays and optimize the scheduling of flights on the runways. Concurrently, the dynamic alteration of runway assignments for flights introduces an additional layer of exploration. This approach facilitates the discovery of optimal or near-optimal solutions.

It is important to highlight that the search space is constrained for both maneuvers. Specifically, when swapping flights, the algorithm focuses solely on flights within a Specified Window (SW) to optimize the model its performance. Similarly, in the case of runway reassignment swaps, the availability of runway ends depends on the operation type, considering that certain runways may not be accessible for either landing or takeoff.

C. Receding Horizon Control

The concept of Receding Horizon Control (RHC) involves breaking down the original problem into smaller subproblems within a sliding time frame, which reduces the computational burden. It relies on two key parameters, the scheduling window time interval and the receding horizon width. Figure 6 shows how RHC works. Within a designated horizon, full optimization is executed utilizing all available information. However, only scheduling decisions on the initial time interval are put into action. By ensuring that the time window for each horizon is significantly smaller than the entire flight schedule, this approach significantly reduces the computational load, enabling faster computations.

When employing the RHC strategy in the FRSM, the problem is divided into several sub-problems by the RHC principle. The number of sub-problems is dependent on the length of the flight schedule. For each sub-problem, information is collected from the start to the end of the window size. The objective function is exclusively applied to the window currently undergoing optimization. For the research shown in this paper, a window size of 30 minutes is chosen with a window shift of 15 minutes.

It is important to know that previous window data contributes to noise and separation considerations. To maintain adequate separation in the current window, the flight schedule from the previous window is essential. Regarding noise, the noise emitted by earlier flights is taken into account. Whenever the window shifts, the noise budget increases by the duration of that shift in seconds. The noise produced by flights that are already optimized guides the starting point for the new optimization at each grid point.

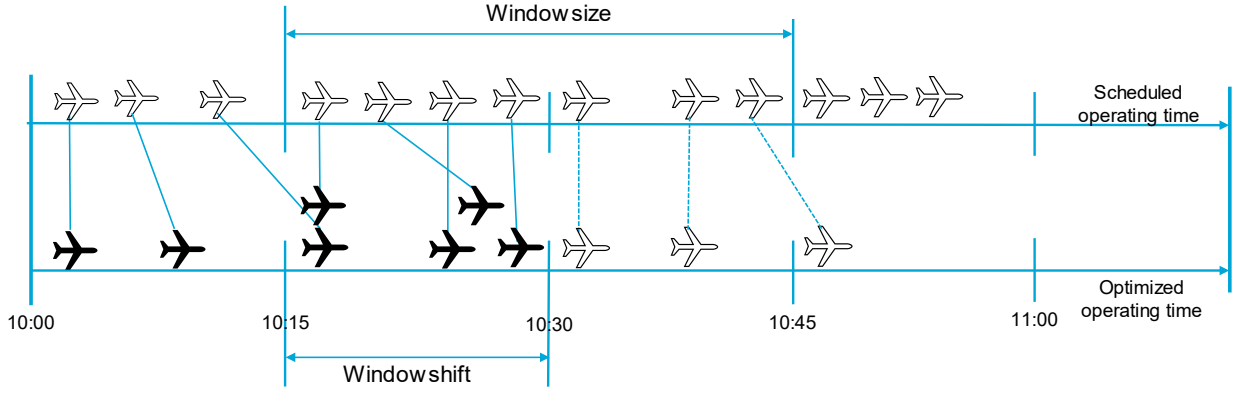

Figure 6: Receding Horizon Control

IV.Case Studies

The analysis of the FRSM utilizes Amsterdam Airport Schiphol (AAS). AAS accommodates a total of 6 runways shown in figure 6, equating to 12 potential runway ends for operations. However, the Oostbaan, encompassing runway ends 04 and 22, is omitted from the analysis as it has a very short runway and is mostly used for General Aviation, private jets, and helicopters. The remaining five runways are strategically oriented to accommodate varying wind directions, ensuring near-constant operability. It is important to note that certain runway ends are restricted for either take-off or landing. Specifically, for departing aircraft, operations are generally limited on the following runway ends: Aalsmeerbaan 36R, Kaagbaan 06, and Polderbaan 18R. Conversely, for arriving aircraft, the following runway ends face operational restrictions: Aalsmeerbaan 18L, Kaagbaan 24, and Polderbaan 36L.

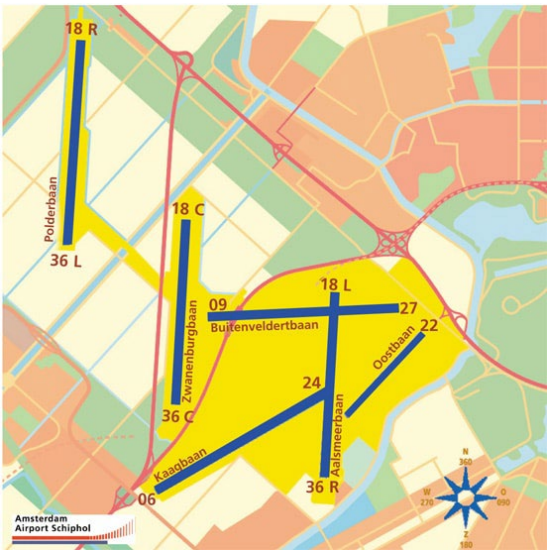

Figure 7: Runways at AMS

For the analysis, multiple flight schedules dated from 2019 are used. These schedules are formulated using authentic flight data extracted from specific days in 2019 and adjusted to function as input for the model. The adjustments involve integrating arrival or departure trajectories based on the designated sector, which relies on the origin or departure data. Additionally, every aircraft is categorized into the correct weight class according to the RECAT-EU regulations[2]. The final stage involves assigning a pier to each flight to facilitate the calculation of taxi fuel consumption, achieved by considering the aircraft type and carrier. The goal of the analysis is to assess how employing an alternative-solving approach impacts the outcomes of the model in contrast to the MILP model. To conduct this comparison, the original MILP model[7] is reconfigured and utilized for the evaluation. The optimization process is conducted using the commercial solver Gurobi. Due to the inclusion of a non-linear element for noise annoyance in the new model, direct optimization of dose response noise objectives is unfeasible as a MILP model cannot handle non-linear elements. Consequently, the LDEN limit for the noise optimization has been established at 48 dB(A). In the event of this limit being exceeded, the total population residing at the respective grid point will be counted. The metric of actual HA people can then be calculated from the optimization results.

The tabu search algorithm is implemented in Python, where multiprocessing is employed to accelerate the optimization process. Specifically, this approach involves parallel computation of the objective function for all generated neighbors in each iteration, significantly enhancing the overall speed of optimization. Four distinct scenarios are considered in the analysis, with an outline of the schedules presented in Table 1. As the flight schedule expands in size, these scenarios reflect varying degrees of complexity. This expansion allows an analysis of both models' behaviors, enabling an observation of how they manage and adapt to the increased volume of flights. The 90-minute scenario originates from Abbenhuis his research appendix dated August 2019, whereas the six-hour scenario spans from August 23, running from 9:00 AM to 3:00 PM. The daytime scenario is drawn from August 20, covering the period from 7:00 AM to 7:00 PM. The full-day scenario originates from July 15, encompassing 24 hours from 00:00 to 23:59. Notably, the noise calculation for this scenario includes an evening penalty applied to flights between 7 PM and 11 PM and a night penalty for flights occurring between 11 PM and 7 AM.

Table 1: Flight schedules created for the analysis

Flight schedule	Total flights	Arriving flights	Departing flights	Schedule duration [hours]
90-minute	122	55	67	1.5
Six-hour	471	180	291	6
Daytime	1,033	511	522	12
Full day	1,508	754	754	24

V.Results

The result are presented in the following manner: firstly, a comparison is made between the objective functions of both models to assess the accuracy of the improved model. Secondly, a comparison of computational times is conducted to determine the impact of the new model on computational performance. To further investigate the computational performance, a convergence analysis is carried out. Following this, the performance of both models on the trade-off is demonstrated through a Pareto Front, after which the noise annoyance and runway allocation are presented. Lastly, a sensitivity analysis is performed for the optimization horizon of the tabu search algorithm.

A. Objective function comparison

To evaluate the performance of both models concerning the main objective functions, a fuel-focused optimization ($\alpha = 1$) and a noise-focused optimization ($\beta = 1$) is conducted. For fuel optimization, this entails the total fuel burn emitted by all flights, while for noise optimization, the metric is the number of HA people. The results are presented in figure 8 for fuel (left) and noise (right). The results show that, for the 90-minute and six-hour scenarios, the MILP outperforms in terms of the fuel consumption objective. Conversely, for the daytime and full-day flight schedules, the tabu search algorithm performs slightly better. Regarding noise optimization, the tabu search algorithm outperforms the MILP in all scenarios. It is essential to mention that the MILP optimization for full-day noise did not converge effectively. Consequently, the obtained solution cannot be considered a genuine comparison. When the process fails to converge effectively, it means it is unable to find an optimal solution within the specified parameters. However, it has been included in the table as a reference point, acknowledging its limitations in convergence.

The variation in the number of HA people across the scenarios can be attributed to several factors. In the first scenario, a notable proportion of Lower Medium weight class aircraft is present compared to the other scenarios. The disparity between the six-hour and daytime scenarios can be allocated to the higher prevalence of aircraft in the upper heavy and lower heavy wake turbulence categories in the six-hour scenario. These aircraft emit more noise, resulting in an elevated count of HA people. Additionally, the full-day scenario contains flights during the evening and night, which incur a noise penalty. This penalty significantly influences the LDEN value, leading to a higher count of HA people compared to other scenarios.

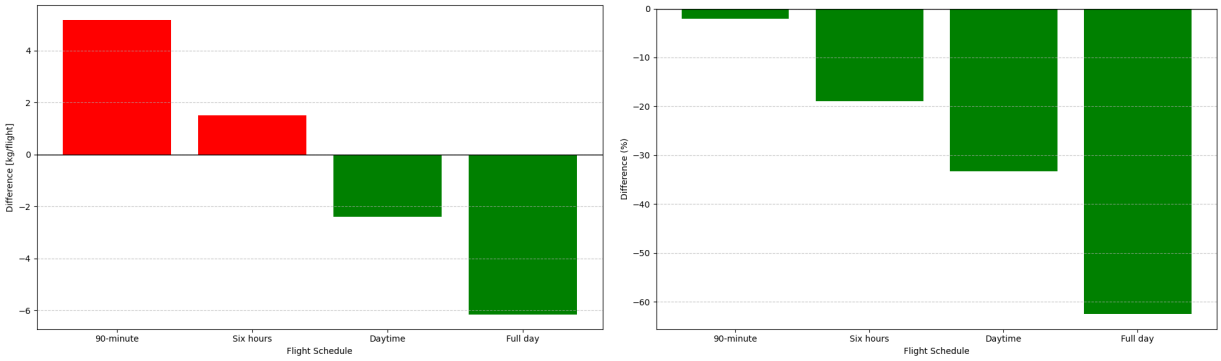

Figure 8: Comparison for fuel (left) and highly annoyed people (right). Green

B. Computational performance

The computational performance of both models is assessed using different methods. The tabu search algorithm allows easy retrieval of computational performance by measuring the time elapsed between the algorithm's initiation and completion. Conversely, the MILP solver continues until the solution converges within a 0% gap range, which is not observed across all the scenarios within a reasonable amount of time. However, to manage computation, a time restriction of 1200 seconds is imposed for the 90-minute flight schedule, while larger scenarios are allocated a time limit of 1800 and 5200 seconds. Additionally, a 7200-second limit is set for obtaining objective values for a comprehensive comparison between fully fuel-optimized and noise-optimized scenarios. These time constraints help regulate and ensure a standardized assessment of computational performance across varied scenarios and models. An overview of the difference in computational time for the tabu search algorithm as the MILP is shown in Figure 9.

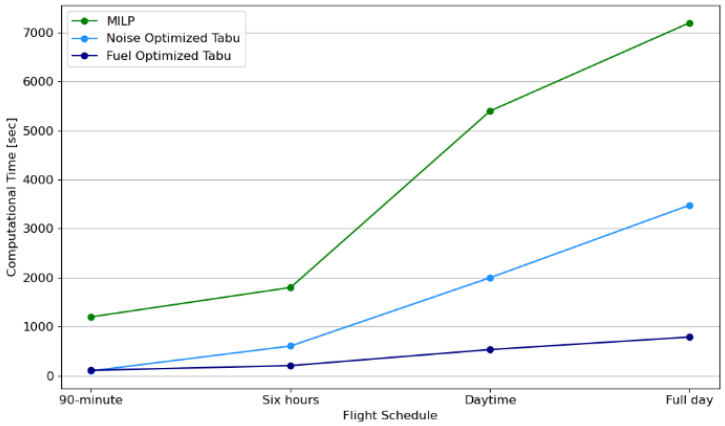

Figure 9: Computational time overview tabu search and MILP for all the scenarios

The correlation between the number of flights in the schedule and the computational time is evident from the figure and flight schedules. The greater the number of flights, the longer the computational time required. For smaller flight schedules, the computational time for noise and fuel optimization falls within a similar range. However, for longer flight schedules, noise optimization consumes significantly more time. This disparity arises from the more extensive noise calculations, necessitating the examination of each neighbor solution across all 900 grid points, which is not required in fuel optimization.

Furthermore, the widening gap between fuel and noise optimization duration can be attributed to the employment of multiprocessing for noise calculations. Multiprocessing efficiency diminishes as data sets expand. The division of work among multiple processors takes longer with larger data sets, contributing to the increasing gap between the longer flight schedules.

Despite the differences in the optimization of both objectives, it can be seen from the figure that they are considerably faster compared to the computational time required for the MILP optimization. However, it is essential to note that these times are user-defined settings, as discussed earlier in this section.

C. Pareto analysis

For visualizing the impact of different weight factors, a series of scenarios were analyzed through the creation of a Pareto Front. This front has been constructed by assigning weights ranging from 0 to 1 in increments of 0.1. Each weight value was utilized to optimize the objective function, thereby enabling the exploration of the relationship between fuel consumption and noise annoyance across various combinations.

To facilitate the selection of the most suitable solution, reference lines for noise and fuel have been plotted. The noise reference line has been derived from the Schiphol 2019 annual report[19], specifically obtained from the recorded number of HA people amounting to 142,000. Conversely, the fuel reference case was generated by optimizing solely for fuel consumption using the original flight schedule and its runway configuration. These reference lines serve as benchmarks against which the Pareto solutions can be compared and evaluated. In figure 10 the Pareto front is plotted for the 90-minute scenario and the six-hour scenario.

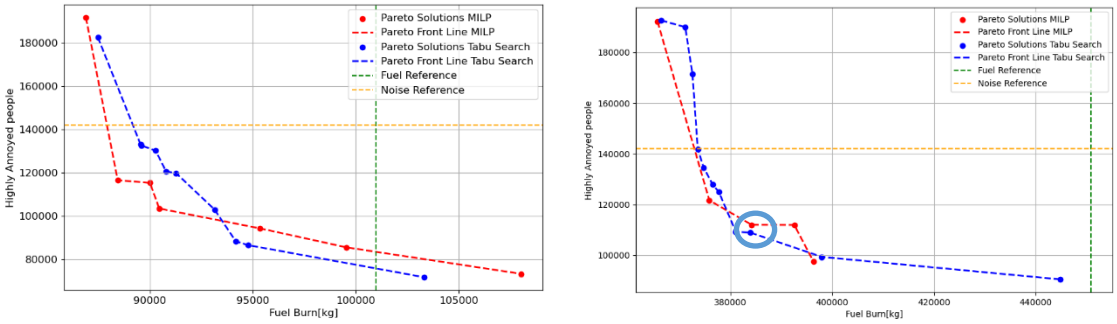

Figure 10: Tabu search and MILP Pareto Front 90-minute (left) six-hour scenario (right)

Comparing both scenarios reveals similarities in the behavior exhibited by the MILP and tabu Pareto plot analyses. In the context of the 90-minute scenario, the tabu algorithm demonstrates superior performance when the focus leans towards optimizing noise. However, this trend shifts when the emphasis moves towards fuel optimization. Notably, both MILP and tabu approaches, exclusively optimizing for noise result in a solution that results in a higher fuel burn compared to the fuel reference scenario. In the case of the six-hour scenario, a more quitable performance is observed, with the tabu search yielding the most optimal solution for complete noise optimization. However, this accomplishment is accompanied by a notable increase in total fuel consumption, albeit still lower than the reference scenario. Importantly, both initial points reside within the boundaries of the fuel reference scenario.

In both scenarios, the tabu search achieves fuel savings compared to the reference scenario for multi-objective weighting. This positioning is near the left bottom of the Pareto curve, ensuring a balance between fuel efficiency and staying below the noise reference limit. The fuel saving can vary from 6.7% for the 90-minute scenario to 15.5% for the six-hour scenario. The difference between the fuel savings can be explained by the investigation of the reference runways, the operation type, and the orientation of the flights. The six-hour scenario contains more departing flights, where more savings can be accomplished compared to arriving flights. Furthermore, the departure trajectories for the 90-minute scenario are mostly located to the south, where already the most fuel-optimal runway is used, which reduces the potential for fuel saving.

In the case of the daytime and full-day scenarios, the MILP approach encountered challenges, failing to converge for various weightings in a reasonable amount of time, thereby hindering the creation of a Pareto plot to depict trade-offs. This again shows the main limitation of the MILP approach, which is the long runtime. Conversely, the tabu search method proved more adaptable to handle these large flight schedules, successfully generating a Pareto plot.

Both Pareto plots indicate that both approaches have their objectives in the same range. However, further analysis is required to determine if the modeling methods make different choices regarding runway allocation. This analysis will be carried out in the next section.

D. Noise Annoyance and Runway Allocation

In this section, an in-depth analysis of the behavior of both models is conducted, centered around the six-hour scenario, incorporating a multi-objective weighting. The selection of this scenario allows a comprehensive evaluation of model performance.

The choice of the point on the Pareto curve, as illustrated in Figure 10, is located close to the left bottom of the curve. The selected point is strategically positioned to achieve simultaneous reductions in fuel burn and noise disturbance. In Figure 12 and Figure 13 the runway allocation and noise annoyance grids of both models are shown for a combination of weights. In Figure 10 the grid points with a population that is Not Highly Annoyed (NHA) are shown in grey.

While the values for fuel burn and the number of HA people exhibit a comparable range for both solutions, several distinctions and similarities can be observed from the graphs. Notably, both solutions demonstrate minimal utilization of runways 18R and 09. The infrequent use of 18R for arrivals is attributed to the extended taxi time required from the runway to the pier, given its location furthest from the gates. Furthermore, the limited usage of 09 for departures can be explained by geographical considerations. Departures in the eastward direction of AAS from this runway are restrained due to the potential for heightened noise annoyance, stemming from the proximity of Amsterdam in that particular area. Upon closer examination, another similarity can be observed in the utilization of runway R36L. Despite its longer taxi time, this runway experiences frequent use, attributed to the advantageous factor of a sparse population situated on its northern side, thereby minimizing noise disturbance. A contributing factor to this preference is the observation that 21% of flights are directed towards the BERGI waypoint, situated in the northern direction. This choice can also be explained by considering alternative northern heading runways. R36C traverses more densely populated areas, and R36R is unavailable for departing aircraft. Consequently, R36L emerges as the preferred runway for flights heading towards the north.

A notable difference between the two solutions can be seen in the utilization of runway 27. The MILP model exhibits a substantially higher usage of this runway compared to the tabu search approach, particularly for arrivals. This higher usage causes an increased noise annoyance over densely populated areas located east of AAS. This discrepancy is further highlighted in Figure 10b, where dark red grid points signify a high concentration of HA people. The tabu search solution, in contrast, opts for alternative runways, mitigating the impact on noise-sensitive regions.

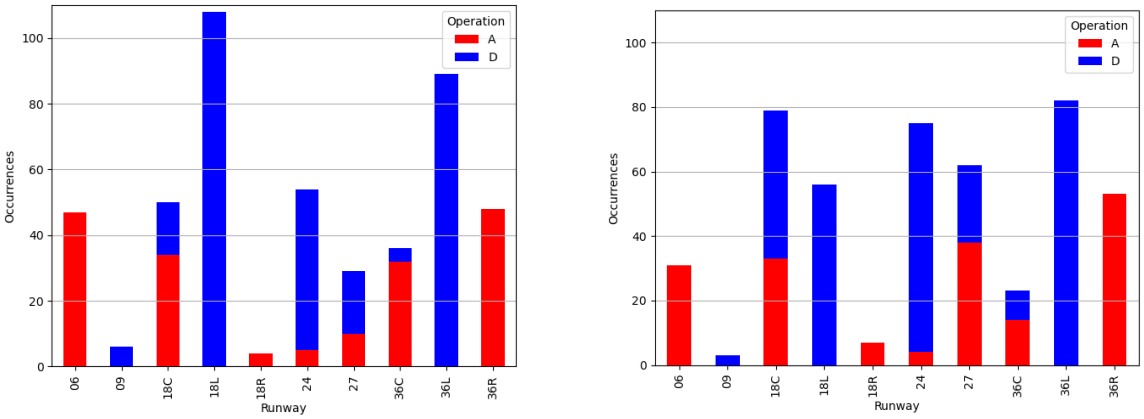

Figure 11: Runway allocation comparison Tabu (left, $\alpha = 0.3$) MILP (right, $\alpha = 0.5$)

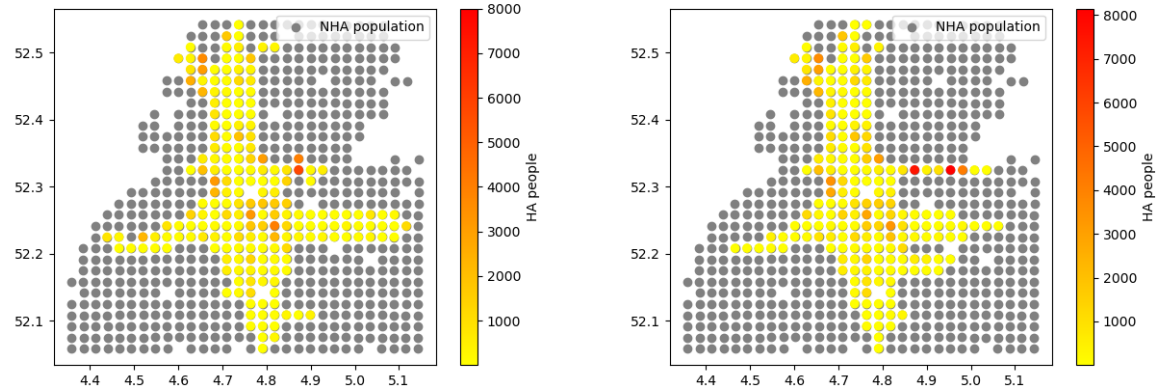

Figure 12: Noise annoyance grid comparison Tabu (left, $\alpha = 0.3$) MILP (right, $\alpha = 0.5$)

Another interesting aspect to explore is the intensity of noise levels experienced by HA people. Given that both optimization models pursue distinct objectives in minimizing noise annoyance, the cumulative count of HA people for each noise level is obtained from the optimization. The results can be seen in Figure 13, revealing variations in the distribution of HA people between the two models.

In both figures, a notable concentration of HA people is observed within the 48-60 dB(A) range. Nevertheless, a noteworthy distinction emerges in the tabu search approach, the majority of HA people experience lower noise levels, while the MILP model exhibits a lower count at the lower noise levels and shows three prominent peaks at higher noise levels. This divergence can be attributed to the fact that, once the noise limit is exceeded, the MILP model no longer considers the intensity of the noise. This results in individuals being exposed to higher noise levels compared to the tabu search. The tabu search, on the other hand, accounts for noise intensity, leading to a decline in the numbers of HA people as noise levels increase. Except for two minor peaks at 63 and 64 dB(A), which can be rationalized by the strategy of avoiding exposure to densely populated areas.

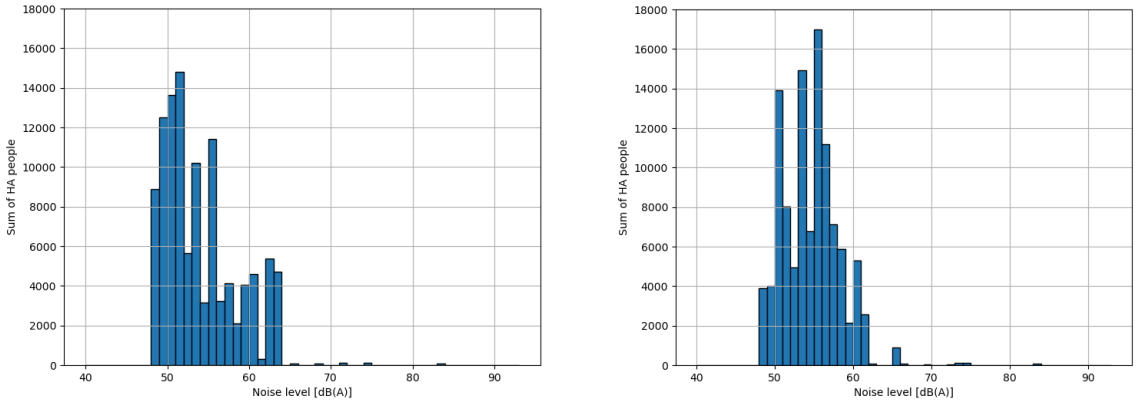

Figure 13: Noise intensity Tabu (left, α = 0.3) MILP (right, α = 0.5)

VI.Conclusions

The aim of this study was to enhance the Flexible Runway Scheduling Model (FRSM) by overcoming two primary limitations, computational performance and simplified noise annoyance modelling. Drawing on the recent model[7], the model was redesigned by incorporating a tabu search optimization technique and integrating receding horizon control to enhance its computational performance. Moreover, the nonlinear nature of noise has been considered, and the number of Highly Annoyed (HA) people has been used as a metric to measure it.

To assess the performance of the tabu search model, four distinct scenarios, varying in the number of flights and complexity have been compared with the MILP model. The results reveal that integrating the tabu search algorithm leads to significant computational savings, ranging from 52% for a noise-optimized full-day flight schedule to 92% for a noise-optimized 90-minute flight schedule. Furthermore, the non-linear noise objective, aimed at reducing noise annoyance, resulted in a significant enhancement, reducing the noise annoyance from 2.14% for the 90-minute schedule to 62.5% for the full-day schedule. However, it is worth noting that for shorter flight schedules, the MILP model outperforms the new model in terms of fuel optimization by 0.73% and 0.19%. This shows that linearization and simplification do affect the results regarding computational performance and noise optimization but have limited influence on fuel optimization.

Both the MILP and tabu search algorithms demonstrated similar results concerning the Pareto front, while the MILP excelled in fuel optimization and the tabu search in noise reduction. The study reveals that reductions in both fuel and noise annoyance are achievable. For the selected 90-minute scenario fuel savings of 6.7% is achievable and for the six-hour scenario 15.5% of fuel savings. Both with a reduction in noise annoyance compared to the 2019 Schiphol reference scenario.

Additionally, the model makes divergent choices when allocating flights to runways, achieving the same results in the objective function. This discrepancy is attributed to the tabu search algorithm incorporating noise annoyance on a non-linear scale, which the MILP model does not account for. The differences between the MILP and tabu search algorithms can be attributed to their respective time horizons. The MILP optimizes the entire flight schedule in one go, while the tabu search uses a moving horizon optimization approach, optimizing smaller segments of the schedule.

To address this variability, variable noise budgets specific to each optimization window are utilized for scheduling the flights. Nevertheless, this approach has a limitation where the model is less effective in allocating flights with sudden spikes in noise levels in the upcoming windows. Despite this limitation, the results show that the majority of HA people experience lower noise levels compared to the MILP approach. This evidence supports the efficient functioning of the non-linear implementation of noise annoyance with variable noise budgets. In summary, this research focuses on an enhanced FRSM, by addressing computational performance and noise annoyance. The research demonstrates that changing the modelling method results in faster computational times and enhances the model its capability to handle larger flight schedules. Additionally, the study highlights the potential benefits of implementing this approach in daily operations. It also indicates positive impacts on the surrounding environment in terms of noise representation and fuel reduction.

VII.Recommendations

While this study employed a tabu search algorithm as a novel optimization technique, exploring alternative optimization methods and evaluating their performance could be valuable. For instance, Multi-Objective Evolutionary Algorithms (MOEAs) present themselves as promising tools adapted to tackling multi-objective functions. The exploration of MOEAs, in addition to the tabu search method, presents an opportunity to potentially improve the problem-solving capabilities of the model concerning multi-objective trade-offs.

An interesting area for future research involves integrating optimal control methodologies to effectively conserve fuel during the aircraft its trajectory. While this study considered fixed-length trajectories for both arrival and departure, existing literature has delved into optimizing either arrival or departure trajectories separately. Incorporating these trajectory optimizations, whether for arrivals or departures, in conjunction with runway scheduling optimizations could yield substantial benefits in further reducing fuel consumption and mitigating noise. Additional resources can be allocated to enhance the modelling of fuel consumption. While this study has already made strides in improving accuracy, further refinement can be achieved by exploring non-linear fuel burn modelling. Incorporating non-linear fuel burn models could significantly enhance the accuracy of the model when simulating real-world data.

A limitation of the current model lies in the fact that it does not consider the runway availability during the allocation of runways to flights. It assumes a best-case scenario where all the runways are available for operations. The user must manually modify the runways restricted for operations. The consideration of wind directions and maintenance of runways is crucial as it impacts aircraft operations, affecting take-off and landing performance. Incorporating real-time or forecasted wind data into the FRSM can optimize the allocation of flights by considering wind direction and intensity. Accounting for wind conditions enables the model to make more informed decisions, such as selecting runways that align favourably with prevailing winds. This could improve aircraft efficiency, and fuel consumption, and potentially reduce noise levels during take-offs and landings.

Lastly, the increased air traffic controller workload should be investigated. Since this model does not consider the additional attention required for constantly switching runways, further research is needed to determine its impact on Air Traffic Management (ATM) systems. The most important parameter for the air traffic controller is to limit the number of runways switching directions.

VIII.References

[1] R. Neufville and A. Odoni. Airport Systems: Planning, Design and Management. McGraw-Hill Education, New York, second edition, 2013.

[2] F. Rooseleer and V. Treve. European Wake Turbulence Categorisation and Separation Minima on Approach and Departure. Technical report, EUROCONTROL, 2015.

[3] J. Hu, N. Mirmohammadsadeghi, and A. Trani. Runway Occupancy Time Constraint and Runway Throughput Estimation under Reduced Arrival Wake Separation Rules. AIAA Aviation 2019 Forum, 2019.

[4] D. Halperin. Environmental noise and sleep disturbances: A threat to health? Sleep Science, 7:209–212, 2014.

[5] Bewoners Aanspreekpunt Schiphol. 2019 Jaarrapportage. Technical report, BAS, 2020.

[6] International Civil Aviation Organization (ICAO). ICAO Doc 9829, Guidance on the Balanced Approach to Aircraft Noise Management. Technical report, ICAO, 2011.IATA fuel price monitor, https://www.iata.org/

[7] Abbenhuis, Anthonie, and Paul C. Roling. "Flexible Runway Scheduling for Complex Runway Systems: Using a Multi-Objective Optimization." AIAA AVIATION 2022 Forum. 2022.

[8] R. Harris. Models for Runway Capacity Analysis. Technical report, The MITRE Corporation, 1972

[9] J. Delsen. Flexible Arrival and Departure Runway Allocation. Master's thesis, Delft University of Technology, 2016.

[10] EUROCONTROL. User Manual for The Base of Aircraft Data (BADA). Technical report, Eurocontrol Experimental Centre, 2004.

[11] Luchtverkeersleiding Nederland (LVNL). Integrated Aeronautical Information Package, 2020.

[12] H. Khadilkar and H. Balakrishnan. Estimation of Aircraft Taxi-out Fuel Burn using Flight Data Recorder Archives. AIAA Guidance, Navigation and Control Conference, 2011.

[13] Kruger-Dokter, A. M., and D. H. T. Bergmans. "Een nieuwe berekeningsmethodiek voor vliegtuiggeluid in Nederland." (2010).

[14] Joey van der Klugt. Calculating capacity of dependent runway configurations. Master's thesis, Delft University of Technology, 2012.

[15] Malcolm J Crocker. Fundamentals of acoustics, noise, and vibration. Handbook of Noise and Vibration Control, pages 1–16, 2007.
[16] C Lee, TT Thrasher, E Boeker, R Downs, S Gorshkov, A Hansen, S Hwang, et al. Aviation environmental design tool (aedt) version 3e technical manual, 2022.
[17] Welkers, D., Sahai, A., van Kempen, E., and Helder, R. (2021). Analyse gelijkwaardigheidscriteria Schiphol. Technical report, Rijksinstituut voor Volksgezondheid en Milieu RIVM.
[18] S.J.Heblij and J.Derei.Methodenrapport doc29. Technical report,National Aerospace LaboratoryNLR, 2019.
[19] Royal Schiphol Group (2020). Annual report 2019.
[20] Glover, F. and Laguna, M. (1998). Tabu search. Springer.